Published online 23 October 2017

Nucleic Acids Research, 2018, Vol. 46, No. 1 ***159–173***
doi: 10.1093/nar/gkx959

Small RNA-mediated Cry toxin silencing allows *Bacillus thuringiensis* to evade *Caenorhabditis elegans* avoidance behavioral defenses

Donghai Peng, Xiaoxia Luo, Ni Zhang, Suxia Guo, Jinshui Zheng, Ling Chen and Ming Sun*

State Key Laboratory of Agricultural Microbiology, College of Life Science and Technology, Huazhong Agricultural University, Wuhan 430070, Hubei, China

Received November 09, 2016; Revised October 03, 2017; Editorial Decision October 05, 2017; Accepted October 09, 2017

ABSTRACT

Pathogen avoidance behavior protects animal hosts against microbial pathogens. Pathogens have evolved specific strategies during coevolution in response to such host defenses. However, these strategies for combatting host avoidance behavioral defenses remain poorly understood. Here, we used *Caenorhabditis elegans* and its bacterial pathogen *Bacillus thuringiensis* as a model and determined that small RNA (sRNA)-mediated Cry toxin silencing allowed pathogens to evade host avoidance behavioral defenses. The *B. thuringiensis* strain YBT-1518, which encodes three nematicidal *cry* genes, is highly toxic to *C. elegans*. However, the expression of the most potent toxin, Cry5Ba, was silenced in this strain when YBT-1518 was outside the host. Cry5Ba silencing was due to the sRNA BtsR1, which bound to the RBS site of the *cry5Ba* transcript via direct base pairing and inhibited Cry5Ba expression. Upon ingestion by *C. elegans,* Cry5Ba was expressed *in vivo* by strain YBT-1518. Cry5Ba silencing may allow *B. thuringiensis* to avoid nematode behavioral defenses and then express toxins once ingested to kill the host and gain a survival advantage. Our work describes a novel model of sRNA-mediated regulation to aid pathogens in combating host avoidance behavioral defenses.

INTRODUCTION

Pathogen avoidance behavior is a highly important phenomenon across all animal taxa and protects host organisms against microbial pathogens and danger (1–3). A host generally faces the following two choices when challenged by pathogens: combat the threatening organism by erecting a physical barrier or activating physiological or cellular defenses (4–6); or avoid the organism by moving away from pathogen-rich regions. This pathogen avoidance behavior minimizes the risk of infection and economizes host resources (1–3). Therefore, avoidance behavior is critical for the survival of all animals, even human beings, in their natural ecological niches and has affected the evolution of foraging strategies, habitat choice, social interactions and mate choice (3,7,8).

The molecular genetics underlying host avoidance behavior have been partially explored in the nematode *Caenorhabditis elegans*, which is a powerful model for dissecting genetic and biochemical mechanisms in animal hosts (1,3). When *C. elegans* is infected, a complex innate immune response is triggered, involving interconnected signaling cascades such as the MAPK (9) and TGF-ß pathways (10), among others. Furthermore, *C. elegans* has evolved behavioral defenses in response to harmful microbes. For example, *C. elegans* engages in host−protective avoidance behavior in response to pathogen derived molecules such as surfactants (11) and quorum−sensing signaling molecules (12–15). Several distinct mechanisms are involved in pathogen avoidance in *C. elegans*, including G protein-like (16), insulin-like (17), and Toll-like receptor signaling (2), as well as neuronal serotonin- (15) and HECT domain-containing E3 ubiquitin ligase-based pathways (14).

Pathogens have evolved specific strategies in response to such host defenses during coevolution (1,18). However, the mechanisms by which pathogens combat host avoidance behavioral defenses remain poorly understood. Several studies have shown that pathogens deceive *C. elegans* via surface molecule modification to prevent detection (1) or produce certain molecules that attract worms (19).

Bacillus thuringiensis is a Gram-positive, spore-forming soil bacterium that produces parasporal crystal inclusions during the sporulation phase of its growth cycle (20). This bacterium has been used as a specific, safe, and effective bio−insecticide to control various pests and nematodes for >70 years (20). *B. thuringiensis* strain YBT−1518, which encodes three nematicidal *cry* genes, namely, *cry55Aa*, *cry6Aa*, and *cry5Ba*, is highly toxic to *C. elegans*. We pre-

*To whom correspondence should be addressed. Tel: +86 27 87283455; Fax: +86 27 87280670; Email: m98sun@mail.hzau.edu.cn

viously demonstrated that the expression of the *cry5Ba* gene is silenced in this strain (21). However, the underlying mechanisms and ecological significance of this unique phenomenon are still unknown. In this study, we identified that a small RNA (sRNA), BtsR1, mediates Cry5Ba silencing in strain YBT-1518. This silencing results in increased ingestion of strain YBT-1518, and is relieved *in vivo* after the ingestion of strain YBT-1518 by *C. elegans*, to increase toxin expression and kill the host. Our work describes a novel sRNA-mediated strategy employed by pathogens in response to host avoidance behavioral defenses.

MATERIALS AND METHODS

Bacterial strains, plasmids, and cultural conditions

The bacterial strains and plasmids used in this study are listed in Supplementary Table S1. *Escherichia coli* and *B. thuringiensis* were incubated at 37°C or 28°C, respectively, in Luria–Bertani (LB) medium with rotary agitation at 200 rpm. Ampicillin (100 μg/ml) for *E. coli* and erythromycin (25 μg/ml) or spectinomycin (20 μg/ml) for *B. thuringiensis* were added to select the strains harboring certain plasmid.

Caenorhabditis elegans strains and culture

Caenorhabditis elegans was cultured at 20°C using standard techniques as previously described (22). The wild-type strain Bristol N2 (22) was provided by the *Caenorhabditis* Genetics Center (http://www.cbs.umn.edu/CGC/).

DNA manipulation and transformation

DNA manipulation was performed according to the methods described by Sambrook and Russell (23). DNA from gels or PCR products was purified using DNA purification kit (QIAGEN, Shanghai). Primers (Supplementary Table S2) were synthesized, and all constructs were confirmed by Sanger sequencing (AuGCT, Beijing). *Escherichia coli* transformation was performed utilizing a standard chemical-competent method (23), and *B. thuringiensis* was transformed by electroporation as described previously (24).

Microscopy observation

For general observation, after *B. thuringiensis* was grown in LB medium to complete sporulation, the crystals and spores were harvested for fuchsin staining and examined with an optical microscope (Olympus, USA) using an oil immersion lens with 10 × 100-fold magnification. For GFP reporter observation, *B. thuringiensis* was grown in LB medium and the cells were harvested at the vegetative stage and observed under a fluorescence microscope (Primostar-FL2) using an oil immersion lens with 10 × 100-fold magnification.

RNA extraction and transcription analyses

Total RNA was extracted from *B. thuringiensis* strains using TRIzol reagent (Invitrogen, California, USA). RNA samples were treated with DNase I (Roche, Basel, Switzerland), then precipitated with ethanol and re−dissolved in RNase-free water. The purified total RNA was quantified by NanoDrop ND-1000 spectrophotometer (Labtech, Wilmington, MA, USA). The qRT-PCR analysis of *cry5Ba* and BtsR1 was carried out using two-step methods with the primers listed in Supplementary Table S2. 2 μg total RNA from each sample was used for cDNA synthesis with Superscript II reverse transcriptase kit (Invitrogen, Carlsbad, CA, USA). qRT-PCR was then conducted with Power SYBR Green PCR Master Mix in an Applied Biosystems 7300 Real Time PCR System (Applied Biosystems, Foster City, CA, USA). 16S rRNA was used as an internal control. At least three independent biological samples were tested and fold-changes between samples were plotted. The Northern blot analysis of *cry5Ba* and BtsR1 was performed as described by Sambrook and Russell (23) with the probes listed in Supplementary Table S2. The 5′-end FAM-labeled BtsR1 and *cry5Ba* RNA probes were synthesized (AuGCT, Beijing, China). Total RNA per lane (5 μg) was separated on a 1.2% agarose gel, and then transferred to a positively charged nylon membrane and UV-crosslinked. The membrane was blocked and washed, and the labeled RNA was detected with a Typhoon Scanner system (GE, Fairfield, CT, USA). The 16S rRNA was used as a reference. At least three independent biological samples were tested. Data from Northern blot analysis were quantified with ImageJ software (available via http://rsbweb.nih.gov/ij/).

Crystal protein purification and detection

Spore and crystal mixtures were collected and washed as described previously (25). The spore crystal pellets were then resuspended in solubilization buffer (50 mM Na_2CO_3, 25 mM dithiothreitol, pH 10.5) and incubated at 37°C for 2 h. The insoluble material that remained was removed by centrifugation, and the solubilized proteins from the supernatant were analyzed by 10% SDS-PAGE. Cry5Ba expression was detected by Western blot using a Cry5Ba antibody as previously described (26).

Prediction and structural analysis of small RNA BtsR1

We constructed a database that contains all the YBT-1518 intergenic region sequences (IGRs) based on YBT-1518 genome annotation. Among these sequences, the bacterial promoter regions were predicted by BPROM (http://linux1.softberry.com/) and Neural Network Promoter Prediction program (http://www.fruitfly.org/seq_tools/promoter.html); while, the Rho-independent transcription terminators were identified using the TransTermHP program (27). The IGRs that contained potential promoter or terminator were retained as potential sRNAs. We then scanned the retained IGRs database using the coding region and promoter sequences of *cry5Ba* by a local BLASTN program. Finally, a putative sRNA, BtsR1, was predicted that could bind with strong complementarity to the *cry5Ba* mRNA. The transcription start site of BtsR1 were ascertained by 5′ RACE technique using SMARTer® RACE 5′/3′ kit (Clontech, CA, USA) with primer in Supplementary Table S2.

Site-directed mutagenesis of BtsR1

Bases were individually mutated according to the secondary structure of BtsR1, which was constructed online (http://rna.tbi.univie.ac.at/). Each mutated base was encoded on a primer (as shown in Supplementary Table S2), and we applied reverse PCR to obtain a fragment containing the mutated base, then linked the mutated base fragments in parallel with Cry5Ba.

Detection of beta-galactosidase activity

Different *B. thuringiensis* cultures (2 ml) in LB medium were collected at the indicated time points. The β-galactosidase-specific activities were measured according to the previously described method (28). The recombinant strains were cultivated in LB medium at 37°C, and the cultured cells were collected and suspended in 665 μl of Z-buffer and beta-mercaptoethanol, followed by the addition of 55 μl of chloroform and 55 μl of SDS. The mixture was incubated in a 30°C water bath for 5 min and activated with 160 μl of ONPG at 30°C for 90–120 min. The reaction was stopped by adding 400 μl of a 1 M Na_2CO_3 solution; and the action times were recorded. We detected the A_{420} absorbance values of these reagents by ELISA. Finally, A_{420} was converted into Miller units. The assays were conducted in triplicate, and the results were shown as the mean ± SE.

The RNA:RNA EMSA assay

In vitro-transcribed RNAs of pcry5Ba (200 nt, −100 to +100 regions of *cry5Ba* mRNA including the ribosome binding site, RBS) and pcry5BaM (187 nt, −100 to +100 regions of *cry5Ba* mRNA without the predicted 13 base pairs that interact with BtsR1) were created. Full-length BtsR1 RNA was synthesized with a FAM label at the 5′ end (AuGCT, Beijing). RNAs were assessed with an RNA6000 NANO chip on the Agilent Bioanalyzer 2100 system. FAM-BtsR1 (10 nM) was incubated in the presence or absence of pcry5Ba RNA (0, 100, 500, 1000, 1500, 2000, 2500 and 5000 nM) or pcry5BaM RNA (0, 100, 500, 1000, 1500, 2000, 2500 and 5000 nM) for the EMSA reactions, which were performed as previously described (29). Samples were electrophoresed through a 5% Tris/Borate/EDTA (TBE) gel at 200 V for 25 min, and then transferred to a positively charged nylon membrane and UV-crosslinked. The membrane was blocked and washed, and the labeled RNA was detected with a Typhoon Scanner system (GE, Healthcare).

Competitive RNA:RNA EMSA

The RNAs of pcry5Ba and pcry5BaM as well as seven selected ΔBtsR1 mutants were transcribed *in vitro*. FAM–BtsR1 (10 nM) was incubated in the presence or absence of pcry5Ba RNA (0 to 1000 nM) to conduct the competitive EMSA reactions. Then, the seven selected, unlabeled BtsR1 mutants were added into each reaction system at a concentration of 5000 nM to compete with the FAM−BtsR1 interaction with pcry5Ba RNA. Reactions were performed as previously described (Liu et al., 2012). Samples were electrophoresed through a 5% TBE mini-gel at 200 V for 25 min, then transferred to a positively-charged nylon membrane and UV-crosslinked. The membrane was blocked and washed, and the labeled RNA was detected using a Typhoon Scanner system (GE Healthcare).

Construction of the *cry5Ba* deletion mutant strain

DNA fragments corresponding to the regions upstream and downstream of the *cry5Ba* gene in YBT-1518 chromosomal were generated by PCR using the primers listed in Supplementary Table S2. The two amplified fragments were digested with BamHI−XbaI and BamHI−KpnI, respectively, and cloned into the temperature-sensitive plasmid pHT304-Ts. Then, the spectinomycin resistance gene from plasmid pBMB2062 was digested with BamHI and inserted between the above two fragments. The resulting plasmid was transformed into strain YBT-1518 and cultivated in LB medium (containing 25 μg/ml erythromycin) for 8 h. Then, the transformants were cultivated at 42°C for 4 days to eliminate the un-integrated plasmid. Erythromycin-resistant (25 μg/ml) but spectinomycin sensitive (20 μg/ml) colonies were harvested. The correct mutant strain was confirmed by PCR and sequencing (AuGCT, Beijing) and named as YBT-1518(Δcry5Ba).

Construction of the BtsR1 depletion strain

Endogenous BtsR1 was depleted by overexpressing the 5′-UTR of *cry5Ba* mRNA including BtsR1 target region. DNA fragments corresponding to the kanamycin promoter in plasmid pHT315-*papha3′gfp*, the 5′-UTR of *cry5Ba* gene (−100 to +100), and the terminator of the *cry5Ba* mRNA were generated by PCR and then fused together by SOE-PCR using the primers listed in Supplementary Table S2. The fusion gene was confirmed by sequencing (AuGCT, Beijing), then digested with KpnI−BamHI and cloned into pHT304 vector. The resulting plasmid was transformed into strain YBT-1518 to generate the BtsR1 depletion strain YBT-1518(BtsR1-dep).

Nematode bioassays

B. thuringiensis strains against *C. elegans* were tested using bioassays as previously described (30).

Nematode pumping rate assays

Pumping rate assays were conducted as previously described (31) to quantitatively assess the feeding rates of individual animals. L4 animals (20–30) were selected and transferred to mutant or wild-type *B. thuringiensis* plate. The times of pharynx movement (pumps) in 30 s of each animal was observed and recorded using a dissecting microscope after the indicated times. This assay was incubated at room temperature with three independent repeats.

Nematode feeding assays

L4 animals (20–30) were transferred to a plate containing mutant or wild-type *B. thuringiensis* cultures to determine fractions of animals in a population that are feeding. Each

animal was observed by using a dissecting microscope for a maximum of 10 s, and scored as 'feeding' if rhythmical backward movements of the grinder were observed. Otherwise, the animals were recorded as not feeding. This assay was incubated at room temperature and observed after the indicated times. Three independent repeats were performed for each assay.

Nematode chemotaxis assays

Chemotaxis assays were conducted based on standard chemotaxis assay protocols (13,32) with some modification. Briefly, 25 μl of control *B. thuringiensis* suspensions (OD_{600} = 1.0) were placed 1 cm away from the edge of a 9-cm Petri dish filled with NG medium (22). The same amount of a test *B. thuringiensis* suspension was placed on the opposing side and acted as the counter attractant. Approximately 50−200 J4 stage animals were placed at the center of the plate. All nematodes were previously fed on *E. coli* OP50. Plates were then sealed with parafilm and stored at room temperature in the dark. Animals could move freely for 1–2 h before they were immobilized with 1 ml of 10 mM sodium azide applied to the spots of bacteria. In most cases, animals quickly entered one lawn and remained there for the duration of the assay. The number of nematodes at each bacterial spot was recorded. A chemotaxis index was used to score the nematode responses and was calculated as follows: (number of nematodes on the test bacteria – number of nematodes on control bacteria)/total number of nematodes counted. This calculation provided a chemotaxis score ranging from −1.0 (complete repulsion from test bacteria) to 1.0 (complete attraction to test bacteria). A score of ∼0 indicates equal numbers of nematodes on all bacterial spots. Five plates were assessed per replicate, and the procedure was repeated at least thrice.

Growth kinetics of *B. thuringiensis* in *C. elegans*

Doses of approximately 10^3 vegetative cells of different *B. thuringiensis* were fed to L4 worms in 48-well plates. Each treatment of 200 μl/well consisted of 160 μl of S-Medium, 20 μl of L4 N2 worms (∼30−50), and 20 μl of the *B. thuringiensis* cultures. Then, the plates were cultured at 20°C for 24−48 h. Worms were collected, washed (with sterile water three times and M9 buffer three times), and centrifuged at 100 × *g*. Finally, 20 worms from each group were homogenized for 5−10 s to break up the tissues, then the tissues were diluted and spread on plates to count the numbers of *B. thuringiensis*.

Data analysis

Data analyses were performed using SPSS (Statistical Package for the Social Sciences) version 13.0 (SPSS, Chicago, IL, USA), and the mean ± SE are shown. Student's *t*-test were performed for statistical comparisons between two values, and differences were significant at the following thresholds: $*P < 0.05$; $**P < 0.01$; $***P < 0.001$.

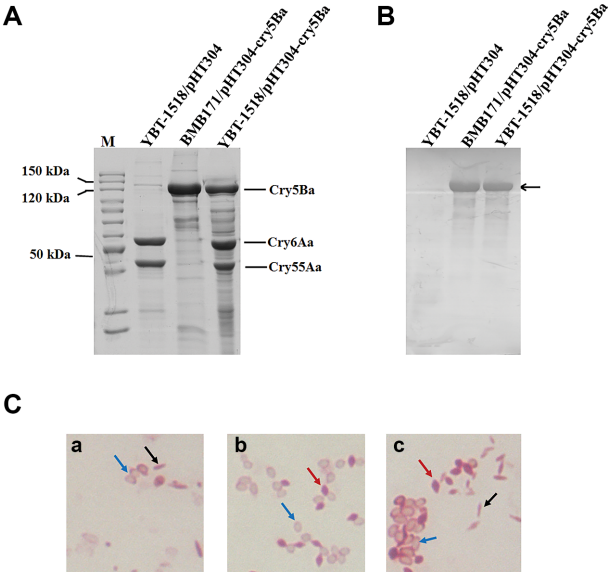

Figure 1. The *cry5Ba* gene was cryptic in *Bacillus thuringiensis* strain YBT-1518. SDS-PAGE (**A**) and Western blot (**B**) analysis detected the expression of Cry5Ba. The total crystal protein samples were prepared from different *B. thuringiensis* strains cultured at 36 h. Line M, molecular mass standard; The black arrows indicate the Cry5Ba protein bands. (**C**) Morphological observation of the crystals produced by different *B. thuringiensis* strains. Panels a, b, c contains crystals produced by strains YBT-1518/pHT304, BMB171/pHT304-cry5Ba, and YBT-1518/pHT304-cry5Ba, respectively. The red arrows indicate bipyramidal-shaped crystals, black arrows indicate rice-shaped crystals, and blue arrows indicate spores. All crystals are observed under an optical microscope and shown at the same magnification (10 × 100-fold).

RESULTS

Nematicidal Cry toxin Cry5Ba was silenced in *B. thuringiensis* strain YBT-1518

In our previous study, we observed Cry5Ba toxin silencing in the strain YBT-1518 (21). We confirmed this observation by evaluating the expression of Cry5Ba in YBT-1518 using SDS-PAGE, Western blot analysis, and microscopy. The expression of Cry5Ba in strain BMB171, which is a crystalliferous mutant of *B. thuringiensis* subsp. *Kurstaki* that does not encode *cry* genes and is nontoxic to nematodes, was used as a control (21). According to the SDS-PAGE results, after growth at 36 h, YBT-1518 produced two major proteins corresponding to the Cry55Aa and Cry6Aa proteins. However, the 140-kDa band for Cry5Ba protein was not detected (Figure 1A). Cry5Ba was also undetectable by Western blot using a Cry5Ba specific antibody (Figure 1B). The expression of Cry5Ba proteins in strain BMB171 results in the formation of bipyramidal-shaped crystals (Figure 1C, panel b). However, microscopic observation only indicated the presence of rice-shaped crystals in YBT-1518 (Figure 1C, panel a), which were formed by Cry6Aa and Cry55Aa (21). These results confirm that the Cry5Ba is silenced in strain YBT-1518.

Cryptic or silent *cry* genes often lack functional promoters (33) or require the help of a downstream gene, ORF2 (34). The *cry5Ba* gene possesses a functional promoter (Supplementary Figure S1), which can drive expres-

sion of *cry5Ba* in strain BMB171 (Figure 1). The *cry5Ba* gene also does not form an operon with other ORFs (Supplementary Figure S2) YBT-1518. We further demonstrated that Cry5Ba silencing is not caused by competition from Cry55Aa and Cry6Aa (Supplementary Figure S3), and does not relate to regulation by flanking sequences (Supplementary Figure S4). Detailed information is described in the Supplementary Information. In this case, the cryptic behavior of Cry5Ba in YBT-1518 appears to be attributable to a mechanism that differs from those mentioned above. When an additional copy of the *cry5Ba* gene was introduced into YBT-1518 via a low copy vector pHT304 under the control of its own promoter, Cry5Ba protein band was detected by SDS-PAGE (Figure 1A) and western blot (Figure 1B). Bipyramidal-shaped and rice-shaped crystals were also observed in the recombinant strain (Figure 1C, panel c). Thus, the cryptic nature of Cry5Ba expression in YBT-1518 was dependent on the copy number of the *cry5Ba* gene.

Cry5Ba silencing in YBT-1518 occurred at the post-transcriptional level

To further understand the mechanisms underlying this silencing, we asked if the regulation occurred at the transcriptional level or a later step. Transcription profiles of *cry5Ba* mRNA in strains YBT-1518/pHT304, YBT-1518/pHT304-cry5Ba and BMB171/pHT304-cry5Ba at different growth phases were assessed by RT-PCR (Supplementary Figure S5) and Northern blot (Figure 2A). The results showed that *cry5Ba* was highly transcribed from stationary phase to late stationary phase (12−36 h) in strains YBT-1518/pHT304-cry5Ba and BMB171/pHT304-cry5Ba. However, *cry5Ba* transcription in YBT-1518 reached the highest levels at 12 h, and then decreased sharply during stationary phase through late stationary phase (16−24 h). These results indicate that c*ry5Ba* transcripts may be destabilized during later growth stages in YBT-1518. To confirm this observation, we perform an mRNA stability assay using rifampicin with the above three strains. The strains were cultured for 16 h, then 100 μg/ml rifampicin was added to stop new transcription. The mRNA of *cry5Ba* was detected by northern blots of total RNA isolated at different times after addition of rifampicin (Figure 2B). The results showed that the half-lives of the *cry5Ba* mRNA in strains YBT-1518/pHT304-cry5Ba and BMB171/pHT304-cry5Ba (with half-life of 5.3 and 5.8 min, respectively) was similar, but was significantly shorter (half-life of 1.0 min) in the strain YBT-1518/pHT304 (Figure 2C).

The expression of Cry5Ba protein in the above strains was also evaluated using Western blot (Figure 2D). Cry5Ba was undetectable at all growth phases in the wild type strain YBT-1518. By contrast, in YBT-1518/pHT304-cry5Ba and BMB171/pHT304-cry5Ba, Cry5Ba was detectable from 12−36 h in very large amounts, which is consistent with the *cry5Ba* transcription profiles in these strains. Thus, the silencing of Cry5Ba expression occurs at the post-transcriptional level in YBT-1518.

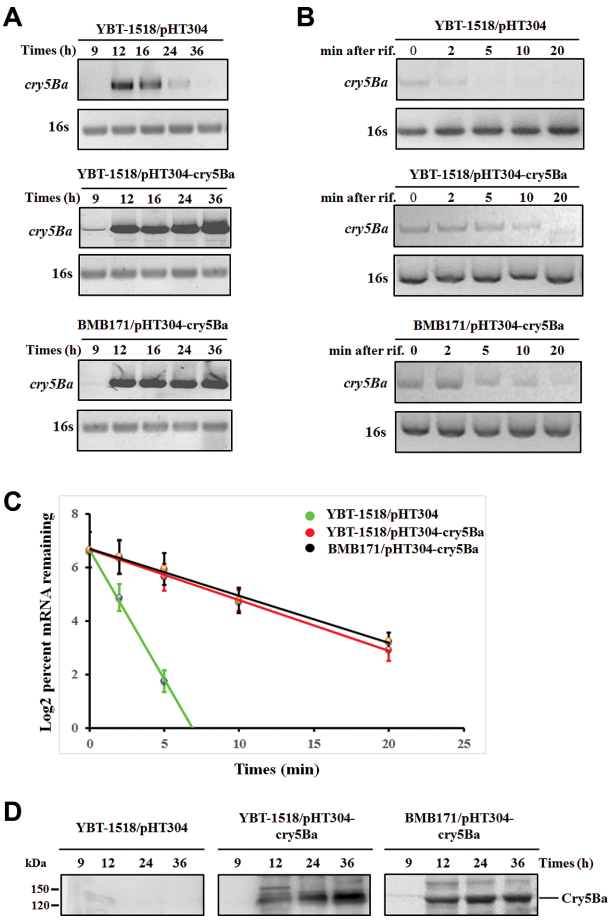

Figure 2. Cry5Ba silencing in strain YBT-1518 occurred at the post-transcriptional level. (**A**) Transcription analyses of c*ry5Ba* mRNA by Northern blot. Total RNA was isolated from *B. thuringiensis* strains from 9 h to 36 h cultured times. (**B**) A representative northern blot showing *cry5Ba* mRNA isolated at times after addition of rifampicin (Rif) to different strains. Rifampicin was added at 16 h cultured times for these strains. The 16S rRNA was used as a reference gene. The relative quantification of the northern blots is presented in (**C**), with the mRNA level at 0 min was set to 100% for each strain. (**D**) Expression profile analysis of Cry5Ba proteins by Western blot. The total protein samples were prepared at different growth phases from cultured *B. thuringiensis* strains. Cry5Ba expression was detected with Cry5Ba antibody.

Cry5Ba was negatively regulated by a small RNA BtsR1

sRNAs negatively regulate the expression of target genes at the post-transcriptional level (35–37). Therefore, we hypothesized that the expression of Cry5Ba may be regulated by specific sRNAs in YBT-1518. Using the YBT-1518 genome sequence (38), we identified a putative sRNA (designated as BtsR1) that could bind with strong complementarity to the *cry5Ba* mRNA. BtsR1 is located on the antisense strand between the *lysR* (encoding a LysR family transcriptional regulator) and *merR* (encoding a MerR family transcriptional regulator) genes. The size of the BtsR1 was predicted to be 51 nt from the transcriptome data of YBT-1518. The transcription start site (+1) of BtsR1 was determined by 5′-RACE (Figure 3A). The targetRNA program (39) gave a high score to a pairing between the BtsR1 intergenic region and the 5′-UTR of *cry5Ba* mRNA. A 13-

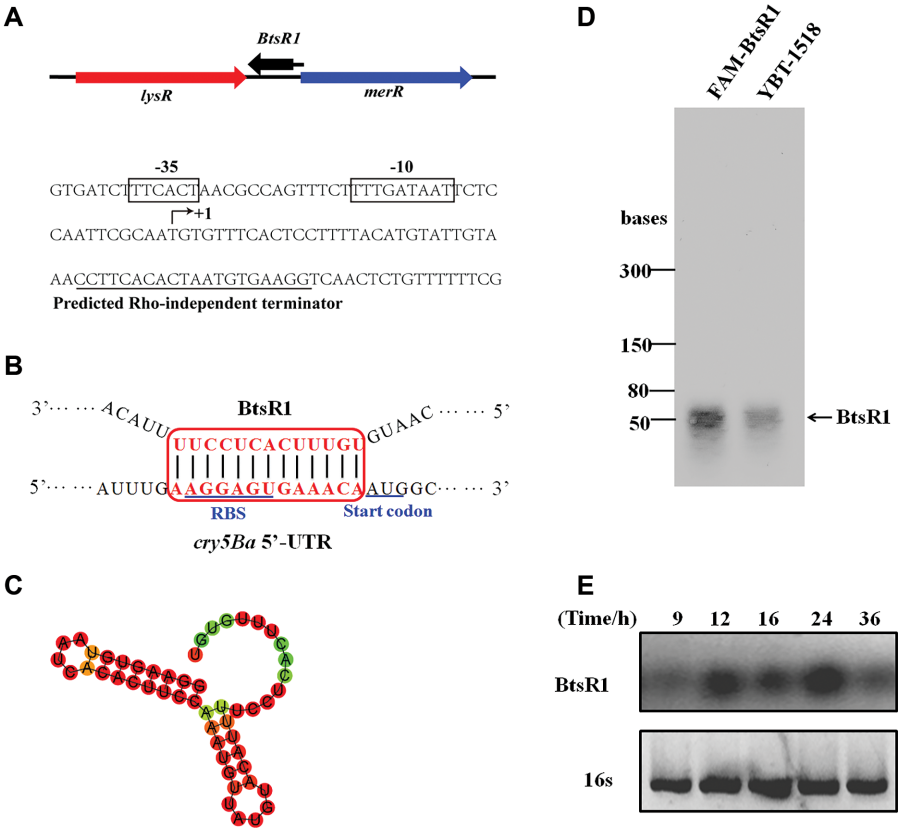

Figure 3. A small RNA BtsR1 in strain YBT-1518 was predicted to target *cry5Ba* mRNA. (**A**) Chromosomal position and sequence analysis of sRNA BtsR1. The transcription start site is indicated by arrows (+1). Putative −10 and −35 regions of the promoters are boxed. The predicted rho-independent terminator is underlined. (**B**) The predicted base-pairing sites between *cry5Ba* mRNA and BtsR1. RBS are underlined. The red box indicates the predicted pairing sites between *cry5Ba* mRNA and BtsR1. (**C**) Predicted structure of BtsR1. The size (**D**) and transcription profiles (**E**) of BtsR1 in YBT-1518 were detected by northern blot. For figure D, total RNA was isolated from YBT-1518 at 24 h growth phase, samples were run alongside RNA markers and the synthesized FAM−BtsR1 with the indicated sizes at the left. For figure E, total RNA was isolated from *B. thuringiensis* YBT-1518 at growth phases from 9 to 36 h. The 16S rRNA was used as a reference gene.

bp sequence in BtsR1 is complementary to the 5′-UTR of the *cry5Ba* mRNA, including the 6-bp RBS (Figure 3B). BtsR1 folds into a stable structure (Figure 3C) with a Gibbs free energy of −14.72 kcal/mol as predicted by the LocARNA tool (40). The putative region of complementarity to the RBS of *cry5Ba* mRNA was in a single-stranded region, which is consistent with the interaction site features reported in the sRNA (41,42). The conservation of the BtsR1 sequence was analyzed using BLASTn against the *Bacillus* genomes deposited in the non-redundant (NR) database. A total of 88 genomes (28 *B. thuringiensis*, 16 *B. cereus*, and 44 *B. anthracis*) contained a BtsR1-like sequence with 100% coverage and 98−100% identity. Within these genomes, the BtsR1 core sequences are highly conserved, except for positions +4, +19, +22 and +47 (Supplementary Figure S6). Interestingly, the predicted *BtsR1*−*cry5Ba* interaction is only observed in *B. thuringiensis* strain YBT-1518, because among the above 88 genomes, only YBT-1518 encodes *cry5Ba*.

We performed a northern blot to determine if the BtsR1 sRNA is produced *in* vivo. Using a BtsR1 specific probe, we detected a transcript consistent with the predicted length (51 nt) of BtsR1 and it showed the same size with that of the synthesized FAM labeled 51 nt BtsR1 (Figure 3D). This result confirmed that BtsR1 is a true sRNA. To check the transcription profile of BtsR1, RT-PCR (Supplementary Figure S7) and northern blot (Figure 3E) were carried out using total RNA isolated from different growth phases of YBT-1518. The results showed that BtsR1 was transcribed from exponential phase to late stationary phase (9–36 h) of growth. However, BtsR1 is not stably transcribed at 9 and 36 h.

To confirm whether BtsR1 inhibited the expression of Cry5Ba, we attempted but failed to construct a BtsR1 deletion mutant strain. Therefore, we constructed a BtsR1 depletion strain by overexpressing the 5′-UTR of *cry5Ba* mRNA including its putative BtsR1 binding site but without the Cry5Ba ORF. BtsR1 levels in the BtsR1 depletion strain are 85−94% lower than wild type (Figure 4A), demonstrating the 5′-UTR of *cry5Ba* can be used to deplete BtsR1. The *cry5Ba* mRNA is more stable when the endogenous BtsR1 is depleted (half-life of 4.8 min), which is significantly longer than that of strain YBT-1518/pHT304 (1.3 min) (Figure 4B). The results of SDS-PAGE and western blot showed that Cry5Ba expressed well when the endogenous BtsR1 is depleted (Figure 4C). We also overexpressed the BtsR1 *in cis* or *in trans* with Cry5Ba (Figure 4D) to confirm whether BtsR1 regulates the expression of

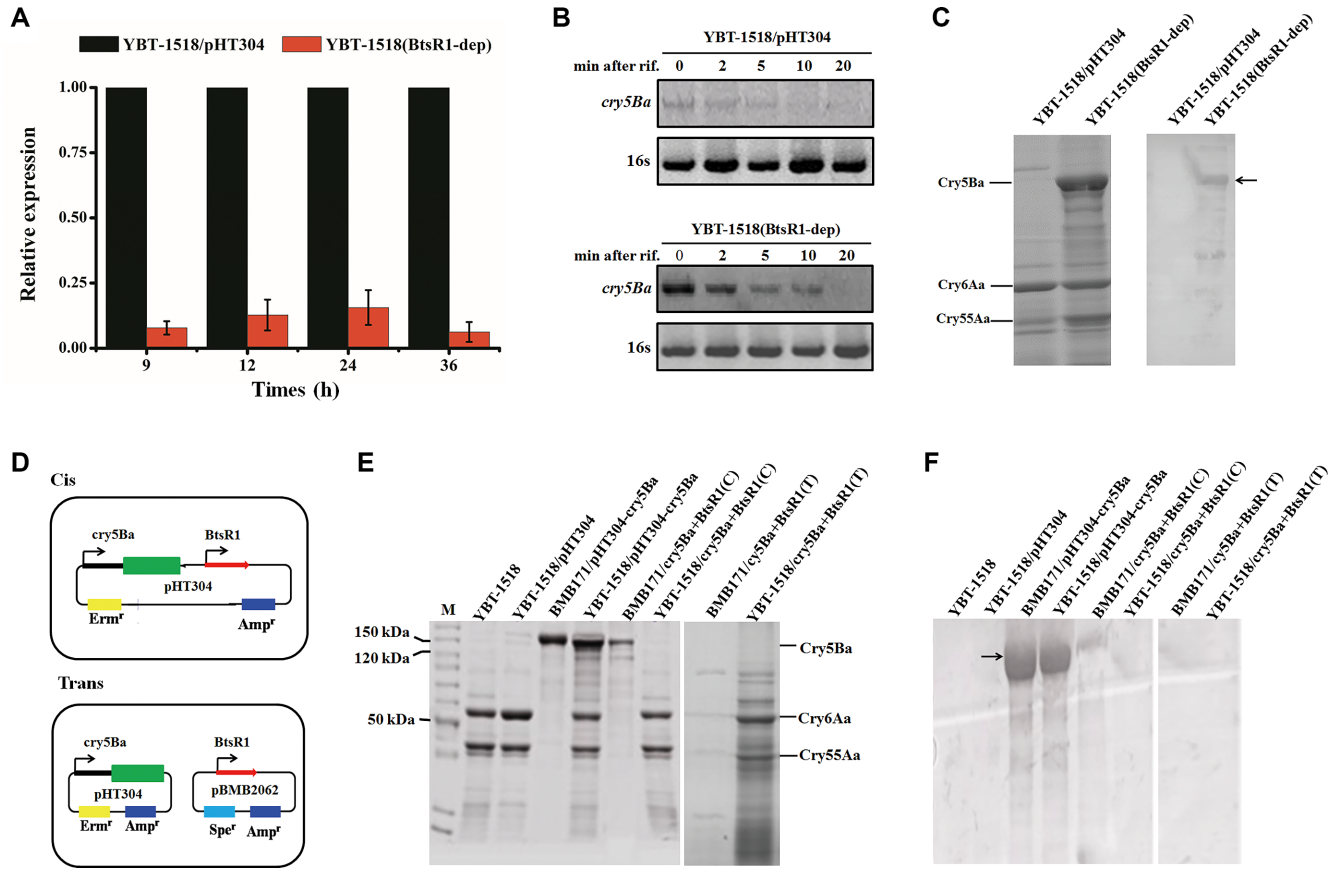

Figure 4. BtsR1 negatively regulated the expression of Cry5Ba in strain YBT-1518 at the post-transcriptional level. (**A**) Transcription analysis of BtsR1 in strain YBT-1518/pHT304 and YBT-1518(BtsR1-dep) as determined by qRT-PCR. Total RNA was isolated after 9 h to 36 h of growth. The 16S rRNA was used as reference gene. The BtsR1 levels in strain YBT-1518/pHT304 at the same time points were set as 1. (**B**) A representative northern blot showing *cry5Ba* mRNA stability in different strains. Rifampicin was added at 16 h cultured times for each strain. The 16S rRNA was used as a reference gene. (**C**) Cry5Ba expression profiles in the wild-type and BtsR1 depletion strain detected by SDS-PAGE (left Panel) and Western blot (right panel). (**D**) Schematic diagram of recombinant plasmid construction to evaluate the *cis*- and *trans*-coexistence of *cry5Ba* and BtsR1 in *B. thuringiensis* strains. Cry5Ba expression profiles in the wild-type and recombinant strains of *B. thuringiensis* were detected by SDS-PAGE (**E**) and Western blot analyses (**F**). The crystal protein samples were prepared from *B. thuringiensis* strains cultured 36 h. Cry5Ba expression was detected with Cry5Ba antibody. The black arrows indicate the Cry5Ba protein bands.

Cry5Ba in the BtsR1 absent strain BMB171 and the wild-type strain YBT-1518. The results showed that either when BtsR1 was expressed *in cis* or *in trans*, Cry5Ba translation in both BMB171 and YBT-1518 was suppressed, as determined by SDS-PAGE. Although a small amount of Cry5Ba expression was still detectable in BMB171, the expression was significantly suppressed compared to expression levels in the absence of BtsR1 (Figure 4E). This finding was further validated by Western blot analysis (Figure 4F). Thus, our data suggests that the sRNA BtsR1 is essential for the negative regulation of Cry5Ba expression in YBT-1518.

BtsR1 directly interacted with *cry5Ba* mRNA by base-pairing with the RBS

The majority of bacterial sRNAs exert their regulatory functions by base-pairing to short stretches within the 5′-UTR of target mRNAs (41,42) to prevent 30S ribosome entry and inhibit translation initiation (37). The predicted interaction region of BtsR1 in the *cry5Ba* mRNA spans a 13-nt 5′-UTR region including the RBS (Figure 3B), indicating that BtsR1 may inhibit the translation initiation of Cry5Ba by base-pairing with its RBS.

To confirm this hypothesis, we used GFP as reporter to test the BtsR1-mediated regulation of the *cry5Ba* mRNA. The *cry5Ba* 5′-UTR was cloned as a translational fusion with *gfp* into the vector pHT315, resulting in pHT315-*pcry5Ba'gfp*. BtsR1 with its own promoter was inserted into the vector pBMB2062. Then, both plasmids were transferred into strains YBT-1518 and BMB171, as shown in Figure 5A. *B. thuringiensis* carrying the plasmid pHT315-*papha3′gfp* (43), containing the *gfp* gene under the control of the constitutive kanamycin promoter, was used as a positive control. We verified GFP protein expression for these strains utilizing fluorescence microscopy. The positive control strains and recombinant strains YBT-1518/pHT315-*pcry5Ba'gfp* and BMB171/pHT315-*pcry5Ba'gfp* showed substantial fluorescence signals after 36 h, compared with the negative control strains which harbored plasmid pHT315. However, no significant fluorescence signals were observed during the same growth phase when both

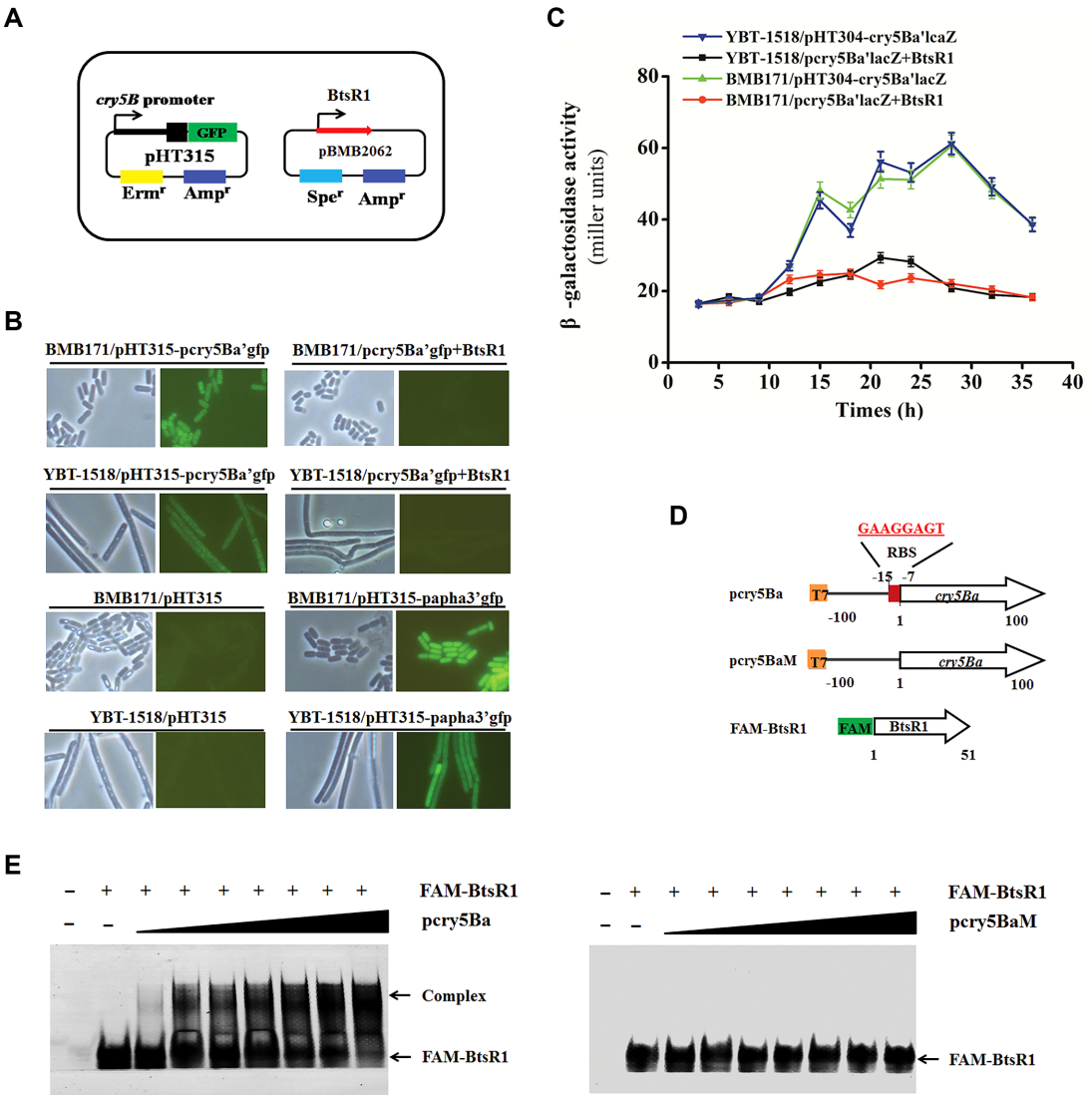

Figure 5. BtsR1 inhibited the initiation of Cry5Ba translation by base-pairing at its RBS. (**A**) Schematic diagram of recombinant plasmid construction using GFP or LacZ as reporter to test the BtsR1-mediated regulation of the *cry5Ba* 5′-UTR. For LacZ, the coding region of *gfp* was replaced with the *lacZ* reporter gene. (**B**) Phase contrast (left panels) and epifluorescence (right panels) microscopy observation of *B. thuringiensis* different carrying different plasmids after 36 h of growth. Green bacteria indicate GFP expression. The host strains are shown at the left. (**C**) The quantitative effects of BtsR1 on the 5′-UTR of c*ry5Ba* as assessed from lacZ fusions. (**D**) The data from the β-galactosidase activity are shown as the average of three independent assays. The error bar indicates the standard deviation (SD). Cells were cultured in LB medium. (**E**) Direct interactions between the BtsR1 and *cry5Ba* 5′-UTR detected by EMSA assay. The wild type (pcry5Ba) and mutant *cry5Ba* 5′-UTR (pcry5BaM) were synthesized via *in vitro* transcription. The 5′-end FAM-labeled BtsR1 (FAM-BtsR1) (10 nM) and increasing concentrations of unlabeled pcry5Ba or pcry5Ba RNAs were hybridized and resolved by native PAGE.

pHT315-*pcry5Ba'gfp* and pBMB2062-BtsR1 were present (Figure 5B).

The effect of BtsR1 on c*ry5Ba* expression was also tested using a *lacZ* fusion. The strains harboring pHT304-*pcry5Ba'lacZ* alone exhibited high beta-galactosidase activity from 12 h to 36 h of growth. The strains harboring pHT304-*pcry5Ba'lacZ* together with pBMB2062-BtsR1 demonstrated significantly lower beta-galactosidase activity at all tested growth phases (Figure 5C) compared to the strains harboring pHT304-*pcry5Ba'lacZ* alone ($P = 0.0021$ in BMB171 background; $P = 0.0024$ in YBT-1518 background, *t*-test). This result indicated that BtsR1 suppressed the expression of *lacZ* under the control of *cry5Ba* promoter. Thus, we concluded that BtsR1 acts on the 5′-UTR of the *cry5Ba* mRNA.

To further confirm that the region in the c*ry5Ba* mRNA targeted by BtsR1 is the RBS, we constructed a mutant *cry5Ba* 5′-UTR lacking the RBS (pcry5BaM) and detected direct interactions in an EMSA assay. The wild-type (pcry5Ba) and mutant *cry5Ba* 5′-UTR (pcry5BaM) were synthesized via *in vitro* transcription (Figure 5D). The 5′-end FAM-labeled BtsR1 (BtsR1-FAM) and increasing concentrations of unlabeled pcry5Ba and pcry5BaM RNAs were hybridized and resolved by native PAGE. FAM-labeled full-length BtsR1 formed higher-molecular-weight complexes with the wild type *cry5Ba* 5′-UTR (pcry5Ba), whereas no shift was observed for the mutant *cry5Ba* 5′-

UTR (pcry5BaM) (Figure 5E). This result indicated that BtsR1 pairs within the *cry5Ba* 5′-UTR region at its RBS. Together, we concluded that BtsR1 interacts directly with the 5′-UTR of *cry5Ba* mRNA by base-pairing at its RBS to inhibit Cry5Ba translation initiation.

Mapping key base-pairing sites in BtsR1 to the RBS of c*ry5Ba* mRNA

To confirm the key base-pairing sites of the BtsR1 interaction with the RBS of c*ry5Ba* mRNA, we applied base scanning mutagenesis and substituted each of the 13 bases in BtsR1 that are predicted to have complementarity to the c*ry5Ba* mRNA (Figure 6A). Each of the BtsR1 variants was cloned into pBMB2062 and transferred into strain YBT-1518/pHT304-cry5Ba. SDS-PAGE was conducted to determine whether mutagenesis influenced the expression of Cry5Ba. Ten of the 13 mutants retained the ability to inhibit Cry5Ba expression; while the other three BtsR1 mutants (BtsR1M5, BtsR1M11 and BtsR1M13, corresponding to the sites of +5, +11 and +13, respectively) lost the ability to inhibit Cry5Ba expression (Figure 6B).

Translational *lacZ* reporter fusions were constructed to confirm these results. Plasmids containing each of the 13 BtsR1 mutants were transferred into strain YBT-1518/pHT304-pcry5Ba'lacZ. The β-galactosidase activities of these recombinant strains were tested in the presence of each BtsR1 mutant. No BtsR1-dependent translational repression was evident in the strains encoding BtsR1M5, BtsR1M11, and BtsR1M13 mutants. However, the strains encoding of the other 10 BtsR1 mutants demonstrated significant inhibition of β-galactosidase activity (Figure 6C). These results identify the bases in BtsR1 relevant for inhibition of Cry5Ba expression.

Competitive EMSA assays were performed to confirm the interactions between the seven selected BtsR1 mutants and *cry5Ba* mRNA. When present at a high concentration (5000 nM), four mutants retained the ability to bind to the *cry5Ba* mRNA, while the other three mutants lost the ability to bind to the *cry5Ba* mRNA. We assessed the ability of the mutants to outcompete the interactions between Cry5Ba mRNA and FAM-labeled BtsR1. The four BtsR1 mutants that retained the ability to inhibit Cry5Ba expression could compete and interrupt the BtsR1-Cry5Ba mRNA interaction, while the three mutants that lost the ability to inhibit Cry5Ba expression exhibited no competition (Figure 6D). These results are consistent with our *cry5Ba* expression studies and the secondary structure prediction results. Thus, the single-stranded-exposed bases of BtsR1 are important for interaction with *cry5Ba* mRNA, and the +5, +11 and +13 sites are the key base-pairing sites for this interaction.

We predicted the secondary structures of all 13 BtsR1 mutants using the LocARNA tool (40). The ten BtsR1 mutants that retained the ability to inhibit Cry5Ba expression folded into stable structures similar to that of wild type BtsR1 (Supplementary Figure S8). In contrast, the secondary structures of the three BtsR1 mutants that lost their ability to inhibit Cry5Ba expression differed compared to that of wild type BtsR1 (Figure 6E). In particular, the predicted single-stranded exposed regions of BtsR1 that are complementary to the RBS of *cry5Ba* mRNA formed a double-stranded stem structure. This change may result in the inability of these three BtsR1 mutants to bind to the *cry5Ba* mRNA. Our results are consistent with previous reports indicating that the single-stranded-exposed bases of sRNAs are more likely to be responsible for regulation than bases in stems (41,42).

Cry5Ba was expressed when YBT-1518 was ingested *in vivo* by nematodes

Strain YBT-1518 has high toxicity to *C. elegans* and possesses three nematicidal *cry* genes, namely, *cry55Aa*, *cry6Aa*, and *cry5Ba* (21). When expressed in strain BMB171, Cry5Ba exhibits the highest activity among these three Cry toxins against nematodes (44). However, the Cry5Ba toxin expression in YBT-1518 is silenced when outside the host (21), and we showed that the sRNA BtsR1 directly binds to *cry5Ba* mRNA and represses the expression of Cry5Ba. This raises the possibility that the Cry5Ba toxin may not contribute to the toxicity of YBT-1518 to the nematode due to the negative regulation by BtsR1. To evaluate whether the BtsR1 mediated Cry5Ba regulation affects the toxicity of YBT-1518, nematode bioassays were conducted with YBT-1518 and BtsR1 mutant strains. To our surprise, YBT-1518 exhibited high toxicity against *C. elegans* N2 similar to those of strains YBT-1518/pHT304-cry5Ba and the BtsR1 depletion strain YBT-1518(BtsR1-dep), in which both express Cry5Ba (*t*-test, $P > 0.05$). Furthermore, the *cry5Ba* knock-out mutant strain YBT-1518(Δcry5Ba) lost most of the toxicity against *C. elegans* N2 compared with that of wild type strain YBT-1518 (*t*-test, $P < 0.001$) (Figure 7A). These results indicated that Cry5Ba is the leading factor for the toxicity of YBT-1518 to nematodes.

The most likely explanation for such situation is that the Cry5Ba may be expressed after YBT-1518 have been ingested *in vivo* by the nematode host, resulting in high toxicity against *C. elegans*. To confirm this hypothesis, we determined the production of Cry5Ba *in vivo* by Western blot. L4 *C. elegans* N2 animals were infected with YBT-1518, YBT-1518/pHT304-cry5Ba, YBT-1518(BtsR1-dep) and YBT-1518(Δcry5Ba), respectively. Then, the bacteria were isolated from 400 to 500 infected *C. elegans* (at 36 hpi) individuals by grinding the worms. The same amounts of bacterial cells cultured in LB medium for 36 h were used as controls. As expected, Cry5Ba was indeed expressed when YBT-1518 in the host, as detected by the presence of the Cry5Ba signal band (Figure 7B).

Then, we compared the BtsR1 transcription profiles in YBT-1518 at different phases during bacterial growth in *C. elegans* and in LB medium by qRT-PCR. For *in vivo* infection, the bacteria were isolated from 400 to 500 YBT-1518-infected *C. elegans* individuals by grinding the worms. The transcription level of BtsR1 under LB medium conditions at the same time points were set to 1. Compared with that in the LB medium condition, BtsR1 showed significant low-level transcription when YBT-1518 was isolated from the host, with downregulation by 141-fold, 187-fold and 351-fold from 12 to 36 hpi, respectively (Figure 7C). Thus, BtsR1 transcription was repressed *in vivo*, which may

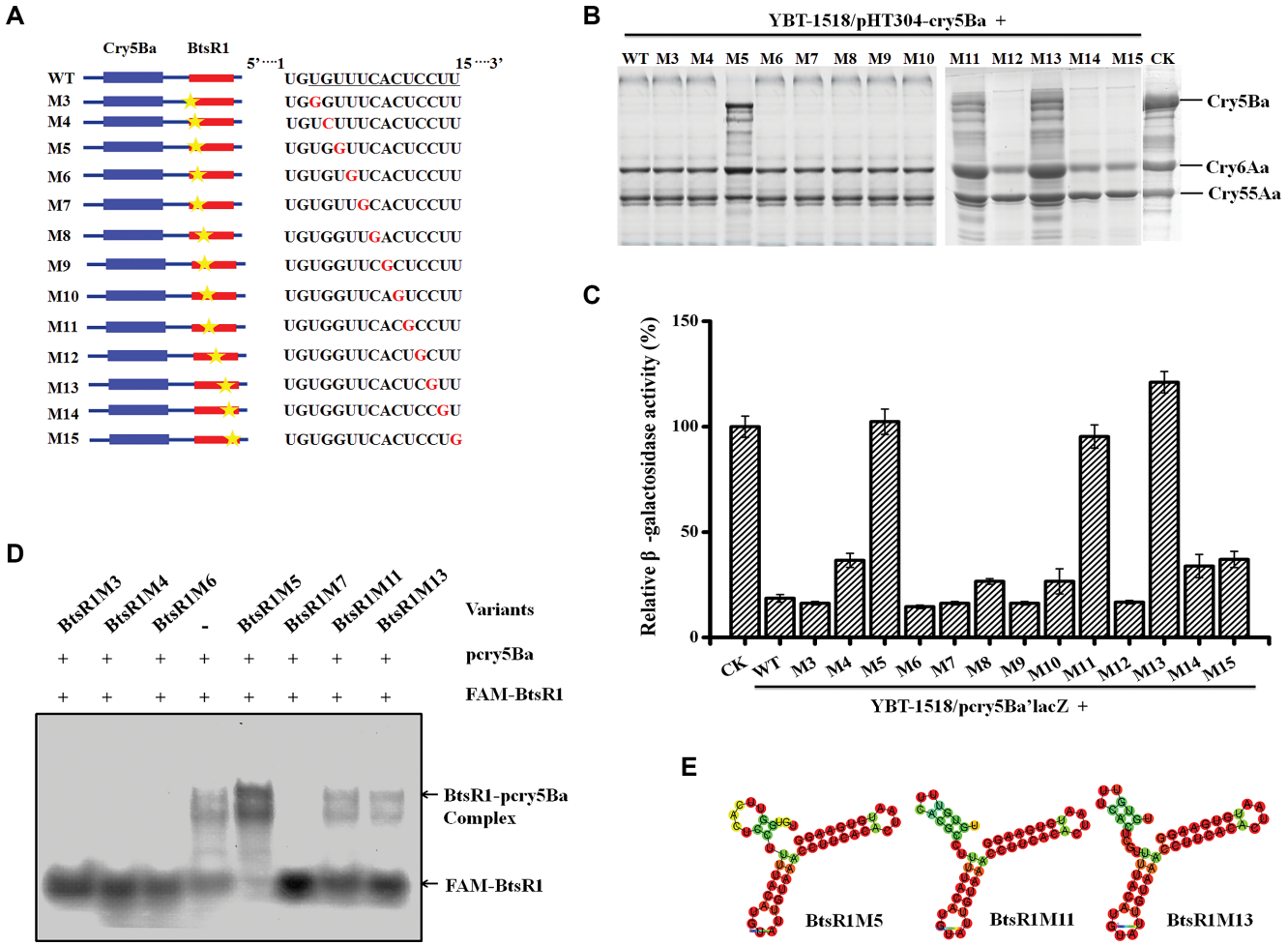

Figure 6. Mapping the key base-pairing sites of BtsR1 to the RBS of c*ry5Ba* mRNA. (**A**) Scanning mutagenesis of BtsR1. The 13 underlined bases in BtsR1 constitute the region that complements c*ry5Ba* mRNA. Red font indicates the mutated base pairs in each mutant. (**B**) SDS-PAGE analysis of Cry5Ba protein expression inhibition by different BtsR1 mutants in strain YBT-1518/pHT304-cry5Ba. The Cry5Ba protein expression in strain YBT-1518/pHT304-cry5Ba are used as a control (CK). The crystal protein samples were prepared at 36 h of growth phase. The positions of the Cry5Ba, Cry6Aa and Cry55Aa protein bands are indicated on the right. (**C**) Translational reporter fusions (lacZ) were performed to confirm the inhibitory functions of BtsR1 mutants. β-galactosidase activity was tested in the presence of each BtsR1 mutant and shown as the average of three independent assays. The β-galactosidase activity of strain YBT-1518/pHT304-*pcry5Ba'lacZ* was used as a control (CK). The error bar indicates the SD. Cells were cultured in LB medium at 24 h. (**D**) Competitive EMSA assay was performed to confirm the interactions between selected BtsR1 mutants and *cry5Ba* mRNA. The wild type *cry5Ba* 5′-UTR pcry5Ba and selected BtsR1 mutants were synthesized via *in vitro* transcription systems. The 5′-end FAM- labelled wild type BtsR1 (FAM-BtsR1, 10 nM) and 1000 nM of pcry5Ba mRNA was hybridized and resolved by native PAGE. Excessive of unlabeled BtsR1 mutants (5000 nM) were used as competitors in these reaction systems. (**E**) Secondary structures of the three BtsR1 mutants that lost the ability to bind *cry5Ba* 5′-UTR.

responsible for the induced expression of Cry5Ba when in the host.

YBT-1518 benefited from BtsR1-mediated Cry5Ba silencing, which facilitated better ingestion and colonization in nematodes

The ability of YBT-1518 to silence Cry5Ba under medium conditions and express this toxin under host conditions is an interesting phenomenon. It has been reported that the Cry5Ba could rapidly induce nematode feeding cessation as an avoidance behavior to this toxin (3,31). Therefore, YBT-1518 potentially silences Cry5Ba toxin expression to confuse *C. elegans*, resulting in host ingestion.

To test this hypothesis, we analyzed the feeding cessation induced by *B. thuringiensis* strains in the presence or absence of Cry5Ba. The strains YBT-1518, YBT-1518(Δcry5Ba), YBT-1518/pHT304-cry5Ba, and YBT-1518(BtsR1-dep) were fed to *C. elegans* N2 L4 animals. Strain BMB171 was used as a control. Pumping rate assays indicate ordinary feeding behavior of *C. elegans* N2 when exposed to BMB171 for 5 min to 2 h and the lack of any significant avoidance. *C. elegans* N2 feeding on strains YBT-1518 and YBT-1518(Δcry5Ba) exhibited only a slight decrease in pumping rate compared to BMB171 at the 5–30 min timepoints (*t*-test, $P<0.05$). However, the feeding behavior of *C. elegans* N2 on YBT-1518/pHT304-cry5Ba and YBT-1518(BtsR1-dep) demonstrated very strong avoidance at all tested time points compared with feeding on BMB171 (*t*-test, $P < 0.001$). The animals ingested the bacteria up to five min, and then all animals ceased feeding between 10 min and 8 h (Figure 8A). The kinetics of feed-

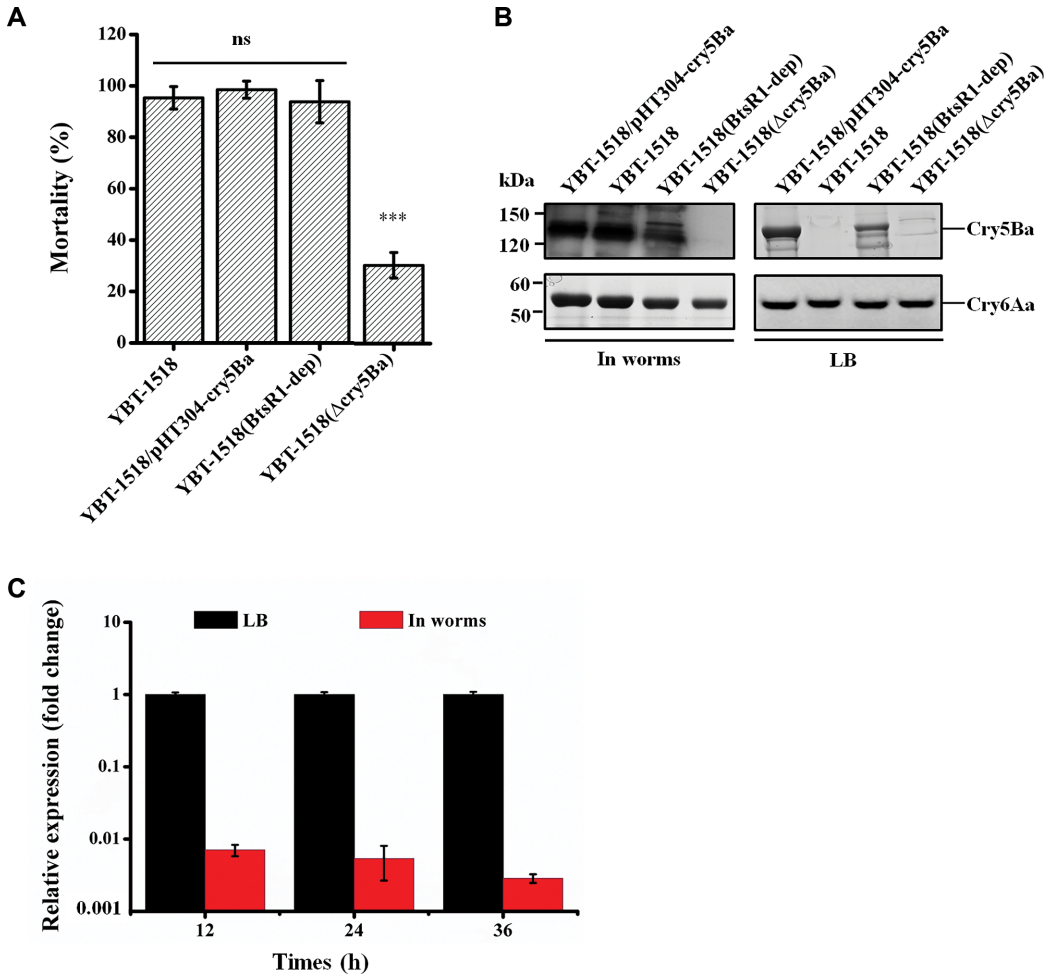

Figure 7. Cry5Ba toxin was expressed *in vivo* when YBT-1518 was ingested by the nematode host. (**A**) Mortality bioassay with different *B. thuringiensis* strains in *C. elegans*. The L4 larvae of wild type *C. elegans* N2 (20-30 for each well) were fed with the same doses of mid-log phase bacteria for the selected strains. Mortality was calculated three days after treatment. Data are presented as the mean ± SE ($n = 3$), and significant differences are as follows: ns, no significant difference; ***$P < 0.001$. (**B**) Cry5Ba expression of different strains under host or LB conditions was detected by Western blot. Total protein samples were prepared from 400−500 N2 animals at 36 hpi. The black arrows indicate the Cry5Ba protein bands detected by Cry5Ba antibody. The expression of Cry6Aa in different strains was detected with Cry6Aa antibody, which was used as loading control. (**C**) Transcription analysis of BtsR1 in strain YBT-1518 under host or LB medium condition as determined by qRT-PCR. For host conditions, RNA was isolated from YBT-1518 infected N2 (400−500 worms) form 12 hpi to 36 hpi. For LB medium conditions, total RNA was isolated from YBT-1518 after 12–36 h of growth. The 16S rRNA was used as reference gene. The transcription levels of BtsR1 under LB medium conditions at the same time points were set as 1.

ing cessation induced by these strains when they were presented as the only food option confirmed the above results. Animal feeding ceased in a significant fraction of the population 5 min after transfer onto YBT-1518/pHT304-cry5Ba and YBT-1518(BtsR1-dep) in the entire population from 30 min to 8 h. No significant feeding cessation at any tested time point was observed in animals exposed to BMB171. When exposed to strains YBT-1518 or YBT-1518(Δcry5Ba), feedings also ceased in a fraction of the population, but this fraction was significantly lower than observed for YBT-1518/pHT304-cry5Ba and YBT-1518(BtsR1-dep) at all tested time points (*t*-test, $P < 0.001$) (Figure 8B). Thus, the BtsR1 mediated Cry5Ba silencing decreases the feeding cessation defense behavior in the *C. elegans* host.

Given that the expression of Cry5Ba by *B. thuringiensis* strains induced more significant host feeding cessation than that of strains without Cry5Ba, we asked which food is preferred by the nematode host when offered jointly. We tested the chemotaxis behavior of *C. elegans* N2 following exposure to *B. thuringiensis* strains with or without the presence of Cry5Ba by a two-choice preference assay (Figure 8C). Two treatments were conducted where YBT-1518 with YBT-1518/pHT304-cry5Ba or YBT-1518 with YBT-1518(BtsR1-dep) were the only food choices. The preference of *C. elegans* for different bacteria was measured in a binary choice assay in which animals migrated towards one of two bacterial lawns on opposite sides of a plate. A choice index of 1.0 represents a complete preference for *B. thuringiensis* strains without Cry5Ba, while an index of −1.0 represents a complete preference for *B. thuringiensis* strains producing Cry5Ba. An index of 0 represents an equal distribution for the two types of bacteria. In both groups, the animals strongly preferred the *B. thuringiensis* strains that did not

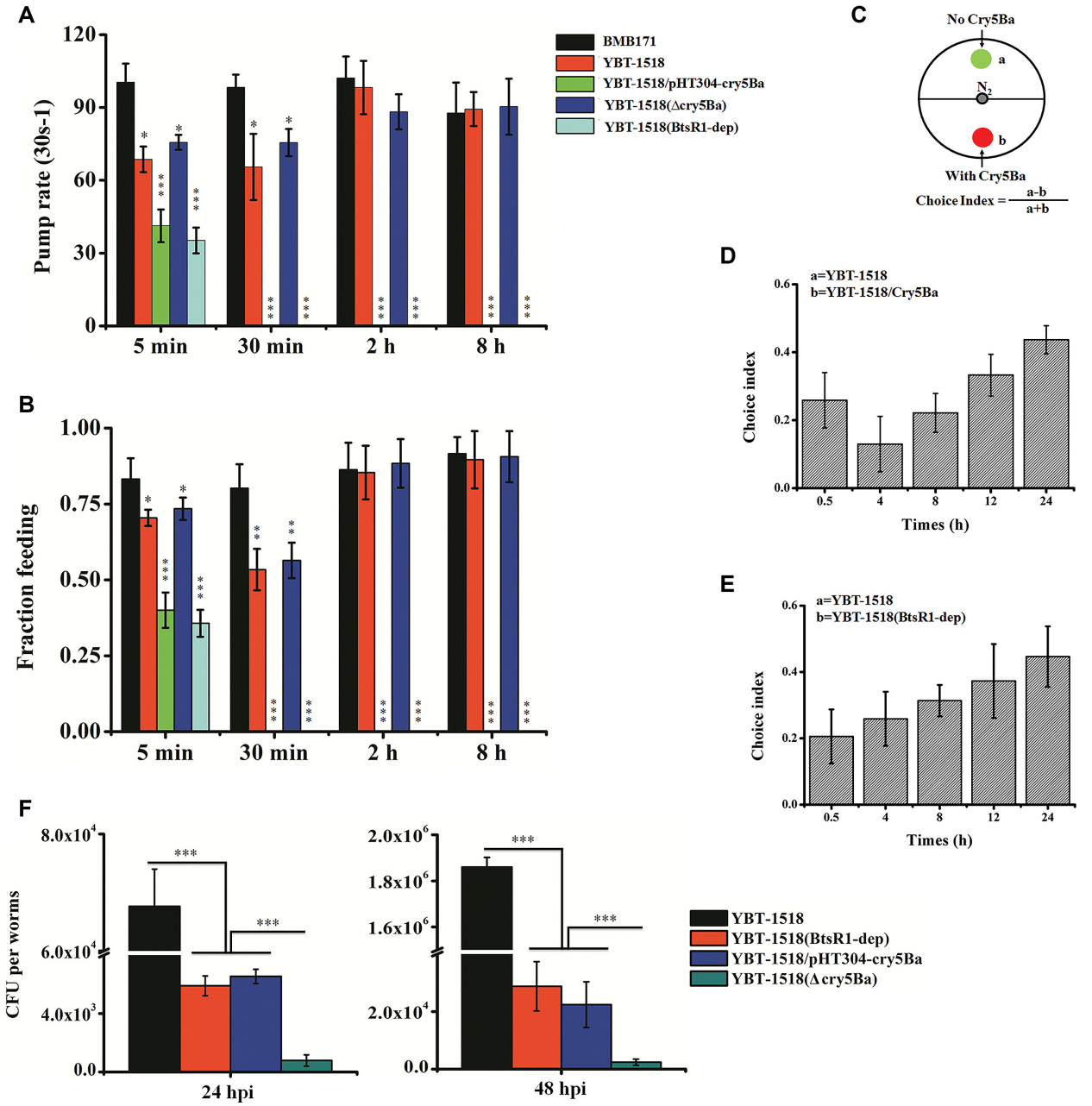

Figure 8. YBT-1518 benefited from the BtsR1 mediated Cry5Ba silencing, which facilitated ingestion by the host and colonization *in vivo*. (**A**) The average pumping rates of animals when exposed to *B. thuringiensis* strains with or without Cry5Ba. (**B**) The fractions of animals that were feeding when exposed to *B. thuringiensis* strains with or without Cry5Ba. (**C**) Schematic representation of the two-choice preference assays. The black dot at the center of the plate represents the starting point of the N2 worms. (**D**, **E**) The worm choice indexes in response to *B. thuringiensis* strains with or without Cry5Ba tested in the two-choice preference assay. (**F**) Cry5B-expressing *B. thuringiensis* results in poor colonization *in vivo*. All data are presented as the mean ± SE ($n = 3$), and significant differences are as follows: $^{*}P < 0.05$; $^{**}P < 0.01$ and $^{***}P < 0.001$. The lack of any symbol indicates no significant difference.

express Cry5Ba (Figure 8D, and E). These results demonstrate that BtsR1-mediated Cry5Ba expression silencing results in a feeding preference for YBT-1518 in *C. elegans*.

We then evaluated the *in vivo* growth of *B. thuringiensis* strains with or without Cry5Ba in *C. elegans* (Figure 8F). After 24 hpi, the population of strains YBT-1518/pHT304-cry5Ba and YBT-1518(BtsR1-dep) were approximately 10-fold (6.54×10^3 cfu per worm) and 11-fold (5.89×10^3 cfu per worm) lower than that of YBT-1518 (6.76×10^4 cfu per worm), respectively. After 48 hpi, the population of *B. thuringiensis* YBT-1518/pHT304-cry5Ba and YBT-1518(BtsR1-dep) showed approximately 83-fold (2.24×10^4 cfu per worm) and 64-fold (2.88×10^4 cfu per worm) lower than that of strain YBT-1518 (1.86×10^6 cfu per worm). The large differential colonization abilities may due to the differences feeding behavior in *C. elegans* following exposure to these strains. Furthermore, strain YBT-1518(Δcry5Ba) could also grow in worms, with populations

significantly lower than that of other strains at same time points (5.01×10^2 and 2.38×10^3 cfu per worm after 24 and 48 hpi, respectively). This result confirmed again that Cry5Ba is the leading toxin, and implies that there are secondary factors affecting the virulence of strain YBT-1518. Anyway, our results showed that BtsR1 mediated Cry5Ba expression silencing increased the odds of *B. thuringiensis* YBT-1518 infecting *C. elegans*.

DISCUSSION

The most intriguing feature of the *B. thuringiensis* strain YBT-1518 is its ability to silence expression of the toxin Cry5Ba during free living growth in medium (Figure 1, (21)) and then to express this toxin when inside a host (Figure 7B). This specialized behavior was mediated by a specific sRNA, BtsR1, which inhibited the expression of Cry5Ba by directly base-pairing with the RBS sites of the *cry5Ba* 5′-UTR (Figures 4-6). Small RNAs are involved in the regulation of gene expression and have been reported in many bacteria to regulate many processes, including DNA replication, nutrient metabolism, oxidative stress, iron homeostasis, toxicity, and persistence (37,41). However, the identification of sRNA and its actions on gene expression has not been reported in *B. thuringiensis*. Our study presents the identification of the first sRNA in *B. thuringiensis,* BtsR1 (Figure 3). In addition, the mechanisms that regulate Cry protein expression in *B. thuringiensis* have been widely studied, and factors such as promoters (45), stable mRNA factors (including STAB-SD sequences (46)), accessory proteins (such as P19 or P20 (47)), and chaperones (including ORF2 (48)) have been identified. Thus far, there has been no report of an sRNA affecting Cry protein expression. Here we showed that an sRNA, BtsR1, bound to the RBS site of the *cry5Ba* mRNA via direct base pairing and inhibited Cry5Ba expression (Figure 4-6). Our present work describes a novel mode of Cry expression regulation mediated by sRNA in *B. thuringiensis.*

The ability of YBT-1518 to silence Cry5Ba under medium conditions and express this toxin under host conditions is a very interesting ecological phenomenon. *C. elegans* is an abundant bacteria-feeding metazoan in soil (49). *B. thuringiensis* has been isolated from diverse environments, primarily from the soil (50). The soil represents a survival space for the coevolution of *B. thuringiensis* and *C. elegans*, and *C. elegans* may provide adequate nutrition for *B. thuringiensis* strains in soil (51). *C. elegans* has evolved certain strategies as defenses against pathogens. One of these strategies involve the evolution of physical barriers, such as the pharyngeal grinder to destroy pathogens (52). Another strategy is the activation of cellular defenses to express AMPs or lysozyme via innate immunity signing pathways such as p38 MAPK (53), JunK-like MAPK (54), and DAF-2 insulin-like growth factor (55). Additionally, *C. elegans* engages in pathogen avoidance behavioral defenses (1,2). As a pathogen, *B. thuringiensis* has also evolved certain strategies to respond to nematodes, such as the formation of spores to escape the pharyngeal grinder or the expression of virulence factors to destroy host physical barriers (44,56). In this study, the ingestion of Cry5B-expressing *B. thuringiensis* resulted in rapid and severe feeding cessation by nematodes (Figure 8A and B), subsequent low levels of feeding preference (Figure 8D and E), and poor colonization ability *in vivo* (Figure 8F), compared to Cry5B-silencing *B. thuringiensis*. YBT-1518 benefited from sRNA-mediated Cry5Ba silencing, which facilitates ingestion by the host (Figure 8D and E) and colonization *in vivo* (Figure 8F). Therefore, YBT-1518 potentially silenced Cry5Ba toxin expression regulated by BtsR1 to subvert *C. elegans* and evade pathogen avoidance behavioral defenses. Indeed, we also demonstrated that YBT-1518 expressed Cry5B *in vivo* (Figure 7B) following ingestion due to a decrease in BtsR1 transcription (Figure 7C). This may allow *B. thuringiensis* to avoid nematode defenses and then express toxins *in vivo* to kill the host and gain a survival advantage. Our work describes a novel mechanism of sRNA-mediated regulation that allows pathogens to combat avoidance behavioral defenses in the host.

Additionally, rich soils harbor large populations of nematodes and microbes, thereby exerting a powerful selective force on both the microbes and nematodes. Given that nematodes demonstrate sensitive avoidance responses, pathogens that gain fitness advantage by infecting the host are selected. These pathogens have evolved certain strategies to conceal their presence, including surface molecule modifications that cannot be detected by host (1) or the production of molecules that attract worms (19). Conversely, selective pressure exists on nematodes to detect this microbial deceit, potentially resulting in a co-evolutionary arms race consisting of repeated cycles of microbial adaptation followed by host counter-adaptation. These dynamics likely shaped both the evolution of the microbe and the host. *B. thuringiensis* produced Cry toxin at a huge cost, both in terms of large pure mass (>25% of the total dry weight of cell) and complex metabolism (57). The production of multiple crystal proteins is energy-consuming but presumably benefits the population by facilitating pathogenic infections (58). There are three crystal protein genes exist in YBT-1518. In this study, the silencing of a specific Cry toxin increases the likelihood of YBT-1518 feeding by nematodes, at least in the context of a recombinant strain producing the Cry5Ba toxin (Figure 8). Cry toxin production is very costly, and hosts represent a fixed pool of resources. Therefore, expression of the Cry toxin solely during the host infection process conserves resources for *B. thuringiensis* survival. Cry5Ba toxin expression in the host and environment mediated by sRNA BtsR1 may be related to reduced fitness costs and derive from host selection, revealing the selective pressures associated with host avoidance behavior that shape pathogen evolution.

In summary, we describe an unusual strain of *B. thuringiensis*, YBT-1518, which possesses the following unique feature: it silenced the expression of the toxin Cry5Ba under medium-growth conditions and expressed this toxin under host conditions. This intriguing regulation represents a new model of pathogen response to host avoidance behavioral defense associated with a novel form of sRNA-mediated regulation of *cry* gene expression. Cry toxin synthesis involved enormous energy consumption by *B. thuringiensis*. Conversion to toxin production in YBT-1518 appears to increase its competitive ability by reducing toxin synthesis in nutritionally deficient environments.

This strategy also allows pathogens to subvert the host and facilitated feeding. After ingestion, the pathogen expressed the toxin *in vivo* to kill the host and obtains a survival advantage. Our work describes a case in which selective pressure associated with a host avoidance behavior shaped pathogen evolution. However, we have not yet to elucidate the host molecules and detailed mechanisms that underlie YBT-1518 sensing and the switch to Cry5Ba toxin production in the host.

SUPPLEMENTARY DATA

Supplementary Data are available at NAR Online.

ACKNOWLEDGEMENTS

We thank Professor Didier Lereclus (INRA, Guyancourt, France) for donation of plasmids pHT315-*papha3′gfp*, pHT304-18Z and pHT315. We also thank Dr Pete Chandrangsu (Cornell University, Ithaca, USA) for critical reading of the manuscript.

FUNDING

National Key R&D Program of China [2017YFD0200400 to D.P. and 2017YFD0201201 to M.S.]; National Natural Science Foundation of China [31670085 to M.S. and 31770116 to D.P.]; China 948 Program of Ministry of Agriculture [2016-X21 to M.S.]; Fundamental Research Funds for the Central Universities [2662017PY094 to M.S. and 2662016PY067 to D.P.]. Funding for open access charge: The National Key R&D Program of China [2017YFD0201201].
Conflict of interest statement. None declared.

REFERENCES

1. Schulenburg,H. and Ewbank,J.J. (2007) The genetics of pathogen avoidance in *Caenorhabditis elegans*. *Mol. Microbiol.*, **66**, 563–570.
2. Brandt,J.P. and Ringstad,N. (2015) Toll–like receptor signaling promotes development and function of sensory neurons required for a *C. elegans* pathogen—avoidance behavior. *Curr. Biol.: CB*, **25**, 2228–2237.
3. Meisel,J.D. and Kim,D.H. (2014) Behavioral avoidance of pathogenic bacteria by *Caenorhabditis elegans*. *Trends Immunol.*, **35**, 465–470.
4. Buchmann,K. (2014) Evolution of Innate Immunity: Clues from Invertebrates via Fish to Mammals. *Front. Immunol.*, **5**, 495.
5. Nakatsuji,T. and Gallo,R.L. (2012) Antimicrobial peptides: old molecules with new ideas. *J. Investigative Dermatol.*, **132**, 887–895.
6. Kugelberg,E. (2015) Macrophages: Controlling innate immune memory. Nature reviews. *Immunology*, **15**, 596.
7. Kavaliers,M. and Choleris,E. (2011) Sociality, pathogen avoidance, and the neuropeptides oxytocin and arginine vasopressin. *Psychol. Sci.*, **22**, 1367–1374.
8. Curtis,V.A. (2014) Infection–avoidance behaviour in humans and other animals. *Trends Immunol.*, **35**, 457–464.
9. Kim,D.H., Feinbaum,R., Alloing,G., Emerson,F.E., Garsin,D.A., Inoue,H., Tanaka–Hino,M., Hisamoto,N., Matsumoto,K., Tan,M.W. and Ausubel,F.M. (2002) A conserved p38 MAP kinase pathway in *Caenorhabditis elegans* innate immunity. *Science*, **297**, 623–626.
10. Gumienny,T.L. and Savage–Dunn,C. (2013) TGF–beta signaling in *C. elegans*. *WormBook*, 1–34.
11. Pradel,E., Zhang,Y., Pujol,N., Matsuyama,T., Bargmann,C.I. and Ewbank,J.J. (2007) Detection and avoidance of a natural product from the pathogenic bacterium Serratia marcescens by *Caenorhabditis elegans*. *Proc. Natl. Acad. Sci. U.S.A.*, **104**, 2295–2300.
12. Beale,E., Li,G., Tan,M.W. and Rumbaugh,K.P. (2006) *Caenorhabditis elegans* senses bacterial autoinducers. *Appl. Environ. Microbiol.*, **72**, 5135–5137.
13. Zhang,Y., Lu,H. and Bargmann,C.I. (2005) Pathogenic bacteria induce aversive olfactory learning in *Caenorhabditis elegans*. *Nature*, **438**, 179–184.
14. Chang,H.C., Paek,J. and Kim,D.H. (2011) Natural polymorphisms in *C. elegans* HECW–1 E3 ligase affect pathogen avoidance behaviour. *Nature*, **480**, 525–529.
15. Aballay,A. (2009) Neural regulation of immunity: role of NPR–1 in pathogen avoidance and regulation of innate immunity. *Cell Cycle*, **8**, 966–969.
16. Bendesky,A., Tsunozaki,M., Rockman,M.V., Kruglyak,L. and Bargmann,C.I. (2011) Catecholamine receptor polymorphisms affect decision–making in *C. elegans*. *Nature*, **472**, 313–318.
17. Hasshoff,M., Bohnisch,C., Tonn,D., Hasert,B. and Schulenburg,H. (2007) The role of *Caenorhabditis elegans* insulin–like signaling in the behavioral avoidance of pathogenic *Bacillus thuringiensis*. *FASEB J.*, **21**, 1801–1812.
18. McLeod,D.V. and Day,T. (2015) Pathogen evolution under host avoidance plasticity. *Proc. Biol. Sci. R. Soc.*, **282**, 20151650.
19. Niu,Q., Huang,X., Zhang,L., Xu,J., Yang,D., Wei,K., Niu,X., An,Z., Bennett,J.W., Zou,C. *et al.* (2010) A Trojan horse mechanism of bacterial pathogenesis against nematodes. *Proc. Natl. Acad. Sci. U.S.A.*, **107**, 16631–16636.
20. Schnepf,E., Crickmore,N., Van Rie,J., Lereclus,D., Baum,J., Feitelson,J., Zeigler,D.R. and Dean,D.H. (1998) *Bacillus thuringiensis* and its pesticidal crystal proteins. *Microbiol. Mol. Biol. Rev.: MMBR*, **62**, 775–806.
21. Guo,S., Liu,M., Peng,D., Ji,S., Wang,P., Yu,Z. and Sun,M. (2008) New strategy for isolating novel nematicidal crystal protein genes from *Bacillus thuringiensis* strain YBT–1518. *Appl. Environ. Microbiol.*, **74**, 6997–7001.
22. Brenner,S. (1974) The genetics of *Caenorhabditis elegans*. *Genetics*, **77**, 71–94.
23. Joseph Sambrook,D.R. (2000) *Molecular Cloning: A Laboratory Manual*. Cold Spring Harbor Laboratory Press, NY.
24. Peng,D., Luo,Y., Guo,S., Zeng,H., Ju,S., Yu,Z. and Sun,M. (2009) Elaboration of an electroporation protocol for large plasmids and wild–type strains of *Bacillus thuringiensis*. *J. Appl. Microbiol.*, **106**, 1849–1858.
25. Shao,Z., Liu,Z. and Yu,Z. (2001) Effects of the 20-kilodalton helper protein on Cry1Ac production and spore formation in *Bacillus thuringiensis*. *Appl. Environ. Microbiol.*, **67**, 5362–5369.
26. Zhang,F., Peng,D., Ye,X., Yu,Z., Hu,Z., Ruan,L. and Sun,M. (2012) In vitro uptake of 140 kDa *Bacillus thuringiensis* nematicidal crystal proteins by the second stage juvenile of *Meloidogyne hapla*. *PLoS One*, **7**, e38534.
27. Kingsford,C.L., Ayanbule,K. and Salzberg,S.L. (2007) Rapid, accurate, computational discovery of Rho–independent transcription terminators illuminates their relationship to DNA uptake. *Genome Biol.*, **8**, R22.
28. Bouillaut,L., Ramarao,N., Buisson,C., Gilois,N., Gohar,M., Lereclus,D. and Nielsen–Leroux,C. (2005) FlhA influences *Bacillus thuringiensis* PlcR–regulated gene transcription, protein production, and virulence. *Appl. Environ. Microbiol.*, **71**, 8903–8910.
29. Liu,Z., Trevino,J., Ramirez–Pena,E. and Sumby,P. (2012) The small regulatory RNA FasX controls pilus expression and adherence in the human bacterial pathogen group A Streptococcus. *Mol. Microbiol.*, **86**, 140–154.
30. Bischof,L.J., Huffman,D.L. and Aroian,R.V. (2006) Assays for toxicity studies in *C. elegans* with Bt crystal proteins. *Methods Mol. Biol. (Clifton, N.J.)*, **351**, 139–154.
31. Los,F.C., Ha,C. and Aroian,R.V. (2013) Neuronal Goalpha and CAPS regulate behavioral and immune responses to bacterial pore-forming toxins. *PLoS One*, **8**, e54528.
32. Bargmann,C.I., Hartwieg,E. and Horvitz,H.R. (1993) Odorant–selective genes and neurons mediate olfaction in *C. elegans*. *Cell*, **74**, 515–527.
33. Song,F., Zhang,J., Gu,A., Wu,Y., Han,L., He,K., Chen,Z., Yao,J., Hu,Y., Li,G. *et al.* (2003) Identification of cry1I–type genes from *Bacillus thuringiensis* strains and characterization of a novel cry1I–type gene. *Appl. Environ. Microbiol.*, **69**, 5207–5211.

34. Barboza−Corona,J.E., Park,H.W., Bideshi,D.K. and Federici,B.A. (2012) The 60−kilodalton protein encoded by orf2 in the cry19A operon of *Bacillus thuringiensis* subsp. *jegathesan* functions like a C−terminal crystallization domain. *Appl. Environ. Microbiol.*, **78**, 2005–2012.
35. Amman,F., Flamm,C. and Hofacker,I. (2012) Modelling translation initiation under the influence of sRNA. *Int. J. Mol. Sci.*, **13**, 16223–16240.
36. Rice,J.B. and Vanderpool,C.K. (2011) The small RNA SgrS controls sugar−phosphate accumulation by regulating multiple PTS genes. *Nucleic Acids Res.*, **39**, 3806–3819.
37. Waters,L.S. and Storz,G. (2009) Regulatory RNAs in bacteria. *Cell*, **136**, 615–628.
38. Wang,P., Zhang,C., Guo,M., Guo,S., Zhu,Y., Zheng,J., Zhu,L., Ruan,L., Peng,D. and Sun,M. (2014) Complete genome sequence of *Bacillus thuringiensis* YBT−1518, a typical strain with high toxicity to nematodes. *J. Biotechnol.*, **171**, 1–2.
39. Tjaden,B. (2008) TargetRNA: a tool for predicting targets of small RNA action in bacteria. *Nucleic Acids Res.*, **36**, W109–W113.
40. Will,S., Joshi,T., Hofacker,I.L., Stadler,P.F. and Backofen,R. (2012) LocARNA−P: accurate boundary prediction and improved detection of structural RNAs. *RNA*, **18**, 900–914.
41. Oliva,G., Sahr,T. and Buchrieser,C. (2015) Small RNAs, 5′ UTR elements and RNA−binding proteins in intracellular bacteria: impact on metabolism and virulence. *FEMS Microbiol. Rev.*, **39**, 331–349.
42. Mars,R.A., Nicolas,P., Ciccolini,M., Reilman,E., Reder,A., Schaffer,M., Mader,U., Volker,U., van Dijl,J.M. and Denham,E.L. (2015) Small regulatory RNA-induced growth rate heterogeneity of *Bacillus subtilis*. *PLoS Genet.*, **11**, e1005046.
43. Daou,N., Buisson,C., Gohar,M., Vidic,J., Bierne,H., Kallassy,M., Lereclus,D. and Nielsen−LeRoux,C. (2009) IlsA, a unique surface protein of *Bacillus cereus* required for iron acquisition from heme, hemoglobin and ferritin. *PLoS Pathogens*, **5**, e1000675.
44. Peng,D., Lin,J., Huang,Q., Zheng,W., Liu,G., Zheng,J., Zhu,L. and Sun,M. (2016) A novel metalloproteinase virulence factor is involved in *Bacillus thuringiensis* pathogenesis in nematodes and insects. *Environ. Microbiol.*, **18**, 846–862.
45. Agaisse,H. and Lereclus,D. (1994) Structural and functional analysis of the promoter region involved in full expression of the cryIIIA toxin gene of *Bacillus thuringiensis*. *Mol. Microbiol.*, **13**, 97–107.
46. Agaisse,H. and Lereclus,D. (1996) STAB−SD: a Shine−Dalgarno sequence in the 5′ untranslated region is a determinant of mRNA stability. *Mol. Microbiol.*, **20**, 633–643.
47. Wu,D. and Federici,B.A. (1993) A 20−kilodalton protein preserves cell viability and promotes CytA crystal formation during sporulation in *Bacillus thuringiensis*. *J. Bacteriol.*, **175**, 5276–5280.
48. Peng,D.H., Pang,C.Y., Wu,H., Huang,Q., Zheng,J.S. and Sun,M. (2015) The expression and crystallization of Cry65Aa require two C−termini, revealing a novel evolutionary strategy of *Bacillus thuringiensis* Cry proteins. *Scientific Rep.*, **5**, 8291.
49. Zhou,J., Li,X., Jiang,Y., Wu,Y., Chen,J., Hu,F. and Li,H. (2011) Combined effects of bacterial−feeding nematodes and prometryne on the soil microbial activity. *J. Hazard. Mater.*, **192**, 1243–1249.
50. Raymond,B., Johnston,P.R., Nielsen−LeRoux,C., Lereclus,D. and Crickmore,N. (2010) *Bacillus thuringiensis*: an impotent pathogen? *Trends Microbiol.*, **18**, 189–194.
51. Ruan,L., Crickmore,N., Peng,D. and Sun,M. (2015) Are nematodes a missing link in the confounded ecology of the entomopathogen *Bacillus thuringiensis*? *Trends Microbiol.*, **23**, 341–346.
52. Labrousse,A., Chauvet,S., Couillault,C., Kurz,C.L. and Ewbank,J.J. (2000) *Caenorhabditis elegans* is a model host for *Salmonella typhimurium*. *Curr. Biol.*, **10**, 1543–1545.
53. Huffman,D.L., Abrami,L., Sasik,R., Corbeil,J., van der Goot,F.G. and Aroian,R.V. (2004) Mitogen−activated protein kinase pathways defend against bacterial pore−forming toxins. *Proc. Natl. Acad. Sci. U.S.A.*, **101**, 10995–10000.
54. Kao,C.-Y., Los,F.C.O., Huffman,D.L., Wachi,S., Kloft,N., Husmann,M., Karabrahimi,V., Schwartz,J.-L., Bellier,A., Ha,C. *et al.* (2011) Global functional analyses of cellular responses to pore-forming toxins. *PLoS Pathogens*, **7**, e1001314.
55. Chen,C.-S., Bellier,A., Kao,C.-Y., Yang,Y.-L., Chen,H.-D., Los,F.C. and Aroian,R.V. (2010) WWP−1 is a novel modulator of the DAF-2 insulin-like signaling network involved in pore-forming toxin cellular defenses in *Caenorhabditis elegans*. *PLoS One*, **5**, e9494.
56. Luo,X., Chen,L., Huang,Q., Zheng,J., Zhou,W., Peng,D., Ruan,L. and Sun,M. (2013) *Bacillus thuringiensis* metalloproteinase Bmp1 functions as a nematicidal virulence factor. *Appl. Environ. Microbiol.*, **79**, 460–468.
57. Agaisse,H. and Lereclus,D. (1995) How does *Bacillus thuringiensis* produce so much insecticidal crystal protein? *J. Bacteriol.*, **177**, 6027–6032.
58. Raymond,B., West,S.A., Griffin,A.S. and Bonsall,M.B. (2012) The dynamics of cooperative bacterial virulence in the field. *Science*, **337**, 85–88.